

# Astronomical Imaging and Image processing.

Jeffrey J Stanger

*Undergraduate Student of the Department of Physics, Macquarie University, Sydney, New South Wales 2109, Australia*

**A correction method is described in which an astronomical image captured using charge coupled device (CCD) can be corrected for common defects. These defects arise both due to the optical path and detection process involved. Digital image processing was carried out using the Mira AP software package and involved correction using dark and flat field images. The method outlined yielded significantly corrected images but the techniques require more investigation to yield optimal results.**

## INTRODUCTION

The field of optical astronomy has undergone a revolution with the development photosensitive arrays called Charged Coupled Devices (CCD). These detectors have replaced traditional methods of astronomical imaging such as photographic plates due to their inherent advantages. These advantages include the lack of reciprocity failure, high quantum efficiency, broad spectral response, increased signal to noise ratio and the efficiency of digital image processing<sup>9</sup>.

The main principle of CCD operation involves the formation of an electron hole pair within a silicon (p-type) semi-conductor by incident photons. The electron hole pairs that are created are attracted to a positive electrode on the surface of the CCD chip and are stored within a potential well during an exposure<sup>9</sup>. This exposure process is depicted below in figure 1 and shows three pixels within a CCD array.

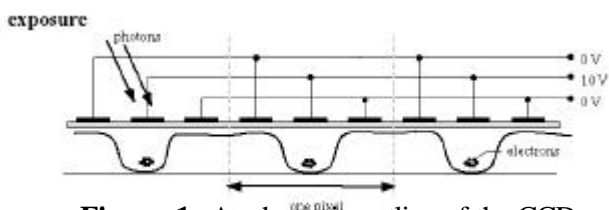


**Figure 1:** A schematic outline of the CCD exposure process.

The accumulated electrons stored in these potential wells of each pixel are 'read' off the array using changing potential gradients across the pixels in the charge transfer stage. The resulting analogue electrical signal from each pixel is converted to a digitised format and downloaded to a computer<sup>9</sup>.

Obtaining accurate astronomical images from the digital output of a CCD involves several corrections using digital image processing. These corrections are necessary due to alterations of the image both within the light path and within the detection procedure itself<sup>8</sup>. The process by which these corrections are carried out involves the acquisition of several reference images and their application to the 'raw' image. A suitable procedure generally involves the removal of image defects or variations in the opposite order to which they were introduced<sup>4</sup>. Such a process is depicted by Equation 1 and represents the method undertaken within this experiment.

$$\text{Final Image} = \frac{\text{Raw Image} - \text{Dark Field}}{\text{Flat Field}} \quad (1)$$

The dark field is an image taken when all light is excluded from the optical system. This exposure corrects for effects within the CCD itself, known as dark current and bias. Dark current is the thermal noise generated within the CCD and is proportional to a power law of CCD temperature<sup>3</sup>. The bias within an image results from an intentional signal introduction to ensure negative values are not processed in the analogue to digital conversion. Both these effects are removed by the subtraction of the dark field from the raw image<sup>1</sup>.

Flat fields are images of a uniformly illuminated source such as the twilight sky. These images remove two types of image artefacts that affect the image in mathematically distinct ways<sup>3</sup>. The first of these is vignetting and other effects introduced into the image from the optical path that result in varying illumination patterns. Flat fields are also able to

correct for sensitivity variations, both as a function of position and wavelength throughout the CCD pixel array. The deviations from ‘flatness’ are due to pixel-to-pixel variations in quantum efficiency or blocked columns<sup>4,6</sup>.

It is evident that through a set of very basic procedures it is possible to correct CCD images for a number of effects. Through the use of image processing software it is the aim of this experiment to produce representative astronomical images by collection and application of correction images.

## EXPERIMENTAL SECTION

### Instrumentation and apparatus:

Images were taken using a 16-inch Meade LX-200 Schmidt-Cassegrain telescope coupled with a Meade Pictor 1616 CCD camera. The CCD imager was equipped with a Peltier cooler and for the purpose of imaging the CCD was cooled to 0°C.

Image processing was carried out using the Mira AP Version 6 software package on an IBM compatible computer.

### Procedures:

Several Raw images were taken on October 29<sup>th</sup> 2001 at approximately 10pm of the globular cluster 47 Tucanae (NGC 104) and the emission nebula 30 Doradus (NGC 2070). The calibration images were acquired on October 31<sup>st</sup> 2001, including dark field and flat field calibration images. Manipulation of the raw images to yield the corrected images involved directly subtracting the dark field and then subsequent division by the median stacked normalised flat field.

Image information for both nights observing is summarised below in table 1. Flat field B was constructed from ten 200ms flat field exposures using median stacking and the resulting image was multiplied by five. Following normalisation these processes yielded a median stacked normalised flat with an equivalent integration time of ten seconds.

Object	Position (RA, Dec.)	Exposure Length (s)
47 Tucanae	00 <sup>h</sup> 24 <sup>m</sup> , -72°04'	10
30 Doradus	05 <sup>h</sup> 38 <sup>m</sup> , -69°04'	10
Dark Current	Aperture Cover	10
Flat Field A	Southern Sky	10
Flat Field B (Composite)	Eastern Sky	10

## RESULTS AND DISCUSSION

The general trend in results for both the raw images were identical and these trends are discussed below in terms of the data for the image of 30 Doradus. All graphical plots and statistical data were gathered over exactly the same region of the images. Statistics for the image of 30 Doradus are summarised below in table 2.

Image	Standard Deviation	FWHM	Pixel Value Range
Raw	50.2	0.74	2751-4749
Raw – Dark	40.2	0.002	131-1391
(Raw – Dark) ÷ Flat	42.3	0.03	125-1407
De-speckled	35.7	2.5	456-1231

The gathering of flat and dark fields was not carried out on the same night as the raw images. Correction images such as dark and flat fields should normally be interspersed throughout the acquisition of raw images. This is done in order to account for the temporal variation of image defects<sup>5</sup>. In this case errors have most likely been introduced through the use of these two temporally separated sets of images.

Upon inspection of the images obtained over the two nights of observing a marked darkening of the upper sixth of the image was noticed and even after cropping it can be seen in figure 2

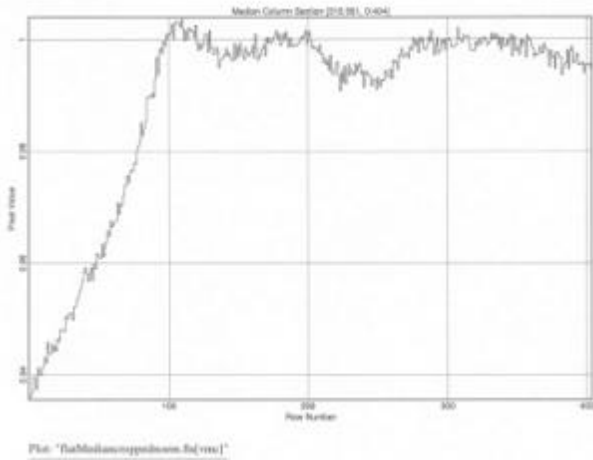


**Figure 2:** Intensity slices of the median stacked normalised flat image.

The darkened region seen above was not observed in the dark field, which is represented by the intensity slice plot below in figure 3.

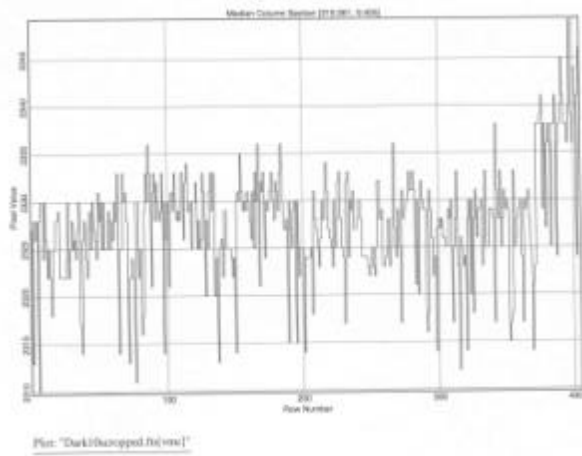


**Figure 3:** Intensity slices of the dark field image.

The dark frame exhibits an approximately uniform distribution thermal noise, with the exception of the bottom of the image. This region does not correspond to the darkened region mentioned above and indicates that the cause of this dark region originates from poor optical alignment or optical path obstruction. Upon application of the correction images it was seen that the corrections did not account for this darkened region in the images. The remnants of this defect can be seen in the top left corner of the inverted image 1 below, as a light region.

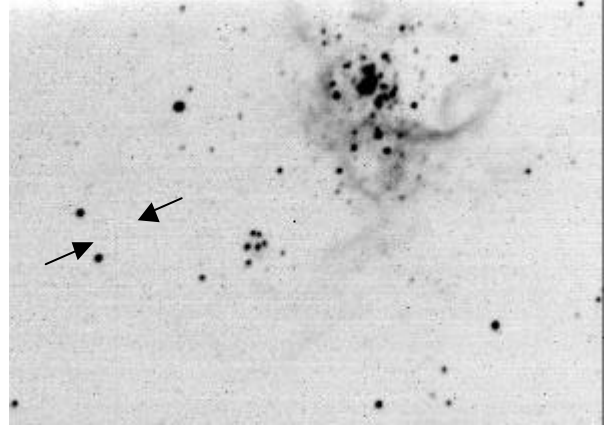


**Image 1 :** Uncorrected and cropped raw image of 30 Doradus.

Upon close inspection of image 1 it is possible to see a large number of ‘hot’ pixels, which are black in this inverted image. These may be caused by defective pixels, excessive thermal noise, cosmic ray strikes or radioactive decay<sup>6,9</sup>. What appears to be an intermittent fault in one of the pixels is indicated between two arrows in image 1. This hot pixel has lead to excess charge being introduced into each pixel’s charge that moved through it in the charge transfer stage of the CCD’s operation<sup>9</sup>. This can be seen as a vertical streak extending from this pixel to the bottom of the image. This effect was only observed on this image and indicates that it is an intermittent fault.

The intensity profile of the raw 30 Doradus image is shown below in figure 4.

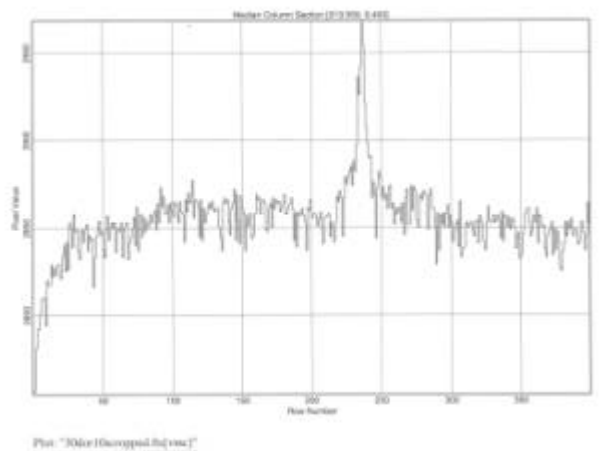


**Figure 4:** Intensity slices of the raw image of 30 Doradus.

Upon subtraction of the dark field from the raw image significant decreases in the standard deviation, FWHM and pixel values can be seen in table 2. The full width at half maximum (FWHM) measurements give a measure of the sky limited resolution<sup>3</sup> or ‘seeing’. Resolution increases when the signal to noise ratio increases and can be seen as a corresponding decrease in the FWHM. The observed decrease in FWHM indicates that the resolution and signal to noise ratio of the image has increased due to the removal of dark current and bias. The image resulting from the dark field subtraction is shown below in image 2.

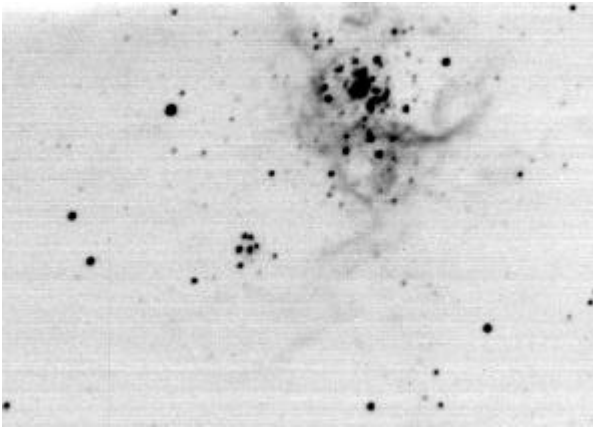


**Image 2:** Dark subtracted image of 30 Doradus.

Several hot and cold pixels can be seen in image 2, indicating that these are due to random errors and may be due to cosmic ray strikes or radioactive decay. The majority of these hot pixels seen in image 1 were removed by the dark subtraction and indicates that they were systematic errors and therefore able to be corrected. The dark subtraction process and resulting rescaling of the intensities in the image resulted in a visible increase in the nebulosity within the image. This demonstrates a qualitative observation of an increase in image quality due to the correction for dark current and bias.

Following this dark subtraction the division of the resulting image by the median stacked normalised flat field image yielded the image shown below as image 3. The effect of this operation can be seen through an increase in the standard deviation, FWHM and pixel values in table 2. This effectively equates to a slight loss of resolution and therefore a drop in the signal to noise ratio.

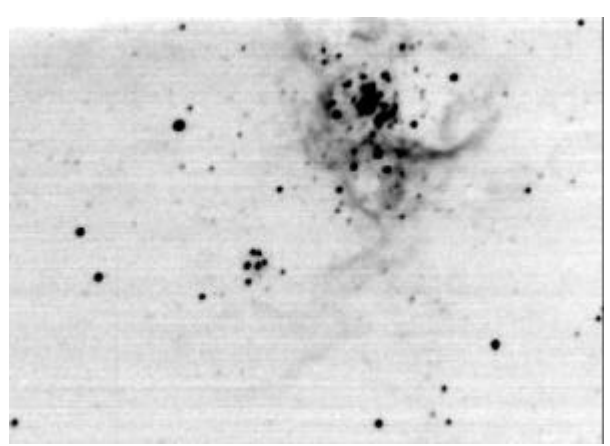


**Image 3:** The dark subtracted and median stacked normalised flat field divided image of 30 Doradus.

In comparison with figure 4, the relative correction of the image to sensitivity and illumination variations due to flat field correction can be observed below in figure 5.

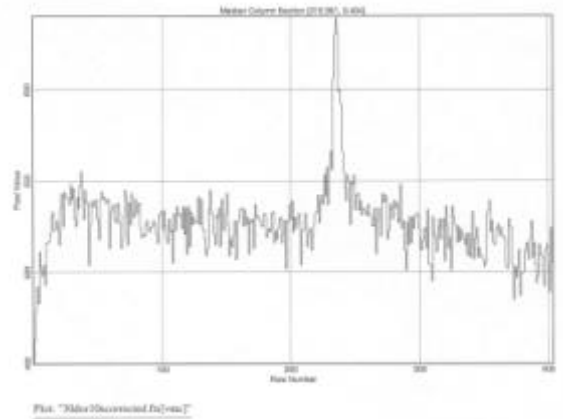


**Figure 5:** Intensity slices of the flat corrected image 3.

The relatively small decreases in signal to noise in images following processing with combined images are due to the nature of noise signals<sup>7</sup>. Noise is random and therefore over a large number of images will tend to cancel. Upon close inspection of image 3, the indication from the data in table 2 is of a loss of resolution is observable as a slight degradation of resolution of the fine nebulosity. Median flats are a good tradeoff between processing complexity and loss of signal to noise as other methods would have lead to a more severely degraded image<sup>4</sup>.

Outliers in the radial plot (Figure 6) illustrate the hot and cold pixels present in the images relative to the point spread function (PSF) from

the source selected<sup>1</sup>. These can be removed by taking several images of an object and median combining them.

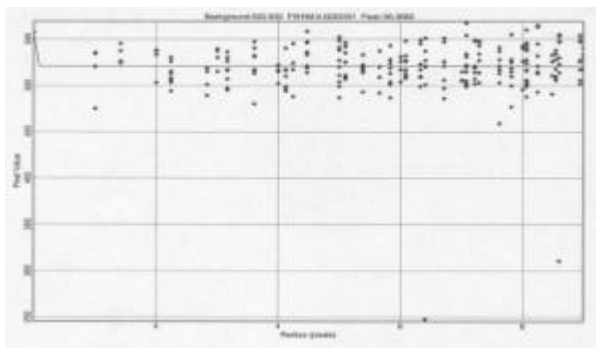


**Figure 6:** A radial plot around a selected source in image 3 shows outliers still present.

Some of the residual image artifacts in the final image would be due to the fact that the calibration images were taken on a different night to the images themselves. Since a CCD temperature difference of as little as 0.2°C could lead to a statistically significant variation in dark count<sup>3</sup>. It is therefore important that dark counts be carried out at regular intervals throughout imaging. Upon close inspection this can be observed as outlier, bright and dark pixels which are removed upon performing a de-speckle filter. The de-speckle function leads to rejection of outliers and therefore removes hot and cold pixels not removed by preceding corrections<sup>1</sup>. This filter was seen to visually improve the image of 30 Doradus (image 4) but degrade the image of 47 Tucanae and therefore was not applied to the latter.

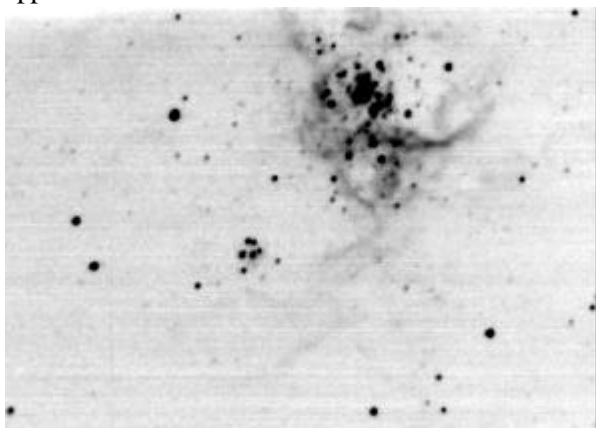


**Image 4:** The de-speckled filtered image of 30 Doradus.

Scaling effects due to the removal of outliers lead to an increase in visible nebulosity in image

4. The actual angular resolution is however much worse and this can be seen also in the FWHM data in table 2.

Further improvements in image quality can be gained through further experimentation with correction images and their application<sup>4</sup>. Since each combination of optical system and CCD are unique it requires experimentation to achieve the best quality images through specific corrections. As noted earlier, significant gains in signal to noise ratio can be made by stacking multiple exposures. Further gains would be made by filtering of light pollution from city lights and would require longer exposures, which inherently increases the signal to noise ratio itself. Investigation into the source of the darkening at the top of the gathered images would lead to either enabling an adequate correction or completely removing the effect.

The raw (Image 5) and median stacked flat corrected (Image 6) images for 47 Tucanae are shown below.

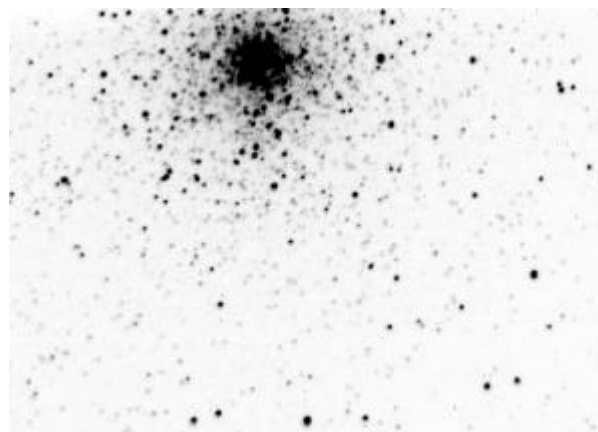


**Image 5:** The raw image of 47 Tucanae.

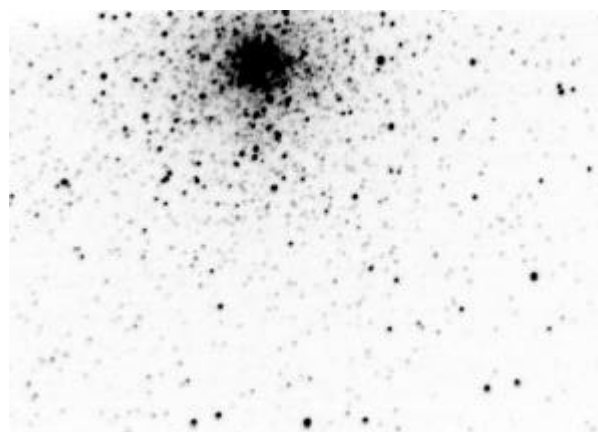


**Image 6:** The median stacked flat corrected image of 47 Tucanae.

These images exhibit similar features as those of 30 Doradus and result in the same image modifications throughout the experiment.

## CONCLUSION

The techniques used in this experiment have illustrated the value that CCD imaging and image processing can bring to astronomy. For example the optical path effects within a telescopic system would not have been able to be corrected using photographic techniques and therein lays a significant advantage. The use of image processing software allowed successful correction of astronomical images was achieved for several common imaging artefacts. The subtraction of dark fields and the division by flat fields allowed corrections for dark current, bias and non-uniform CCD response. These techniques, although yielding significant improvement, still require more investigation to yield optimal results.

## REFERENCES

- (1.) Axiom Research. *Mira AP Image Processing Software, Version 6, Users Guide*. Axiom Research, USA, 2000.
- (2.) Axiom Research. *Online Help*. Accessed at: [www.axres.com](http://www.axres.com) and [axres@earthlink.net](mailto:axres@earthlink.net). (28/11/2001).
- (3.) Axiom Research. *Technical Notes*. Accessed at: [www.axres.com](http://www.axres.com). (26/11/01).
- (4.) Holtzman. J. *Astronomy 535, Observational Techniques, Class Notes*. Accessed at: <http://ganymede.nmsu.edu/holtz/a535/ay535notes/ay535notes.html>. (15/11/01).
- (5.) Lena. P., Lebrun. F. & Mignard. F. *Observational Astrophysics*. 2<sup>nd</sup> Ed. Springer-Verlag, Germany, 1998.
- (6.) Meade. *Meade Pictor XT-series Instruction Manual*. Accessed at: [www.meade.com/manuals/pictor/index.html](http://www.meade.com/manuals/pictor/index.html). (27/11/01).
- (7.) Newberry. M.V. *The Signal to Noise Connection*. Accessed at: [www.skypub.com/imaging/ccd/signalnoise.htm](http://www.skypub.com/imaging/ccd/signalnoise.htm). (26/11/01).
- (8.) Santa Barbara Instrument Group. *CCD Imaging Tutorial*. Accessed at: [www.sbig.com/sbwhtmls/online.htm](http://www.sbig.com/sbwhtmls/online.htm) (27/11/01)
- (9.) Smith. R.C. *Observational Astrophysics*. Cambridge University Press, USA, 2000.